Tellus (1990), *42B*, 118–134

Radon-222 as a test of convective transport in a general circulation model

By DANIEL J. JACOB, *Department of Earth & Planetary Sciences and Division of Applied Sciences, Pierce Hall, 29 Oxford St., Harvard University, Cambridge, Massachusetts 02138, USA*
and MICHAEL J. PRATHER, *Goddard Institute of Space Studies, 2880 Broadway, New York, NY 10025, USA*

(Manuscript received 2 January 1989; in final form 1 August 1989)

ABSTRACT

The distribution of ^{222}Rn over North America is simulated with a 3-d chemical tracer model (CTM) based on the meteorology of the GISS general circulation model (GCM). The GISS GCM has been used extensively for studies of climate change and global transport of chemical tracers. Simulation of ^{222}Rn (*e*-folding lifetime 5.5 days) tests the ability of the model to describe the transport of pollutants in the boundary layer and the exchange of mass between the boundary layer and the free troposphere. Model results are compared to surface observations from 5 sites in the United States. It is found that the ^{222}Rn concentrations are regulated primarily by dry convection. At night, the model underpredicts observations because it does not resolve the sharp ^{222}Rn concentration gradient which forms near the surface. In daytime, the predicted and observed concentrations are usually in good agreement, indicating that vertical mixing of surface air is reasonably simulated. Inspection of seasonal trends reveals, however, several significant discrepancies which are traced to anomalies in the GCM meteorology. In particular, the simulated ^{222}Rn concentrations over the northeastern United States are too high in the spring, because of excessive rainfall which suppresses dry convection, and too low in the fall, because of a severe drought which allows intense dry convection. Ventilation of ^{222}Rn to the free troposphere is most efficient in the western half of the North American continent, due to intense dry convection, and is followed by rapid eastward advection of ^{222}Rn in the upper westerlies. This transport mechanism produces a layer of high ^{222}Rn concentrations in the upper troposphere over the eastern United States and over the western Atlantic Ocean in summer.

1. Introduction

This paper describes a simulation of the atmospheric distribution of ^{222}Rn over North America, using a 3-d chemical tracer model (CTM) based on the meteorology from a general circulation model (GCM) developed at the Goddard Institute of Space Studies (GISS) (Hansen et al., 1983). The CTM has been used previously to simulate the global atmospheric distributions of several long-lived tracers (CO_2, CFC's, ^{85}Kr); good agreement was found with surface observations from sites around the world (Fung et al., 1983; Prather et al., 1987; Jacob et al., 1987). The succesful simulation of long-lived tracers lends confidence in the ability of the CTM to describe interhemispheric exchange and transport between mid-latitudes and the tropics. It encourages investigation of more complex tropospheric problems, such as ozone or acid precipitation, which require a good simulation of transport not just on the global scale but on convective and synoptic scales as well. Study of ^{222}Rn tests the ability of the CTM to simulate transport at that level of detail.

Radon-222 is a radioactive gas (*e*-folding lifetime 5.5 days) emitted ubiquitously by soils. It is a sensitive tracer of vertical transport over continents because its lifetime is of the same order as the time scale for ventilation of the

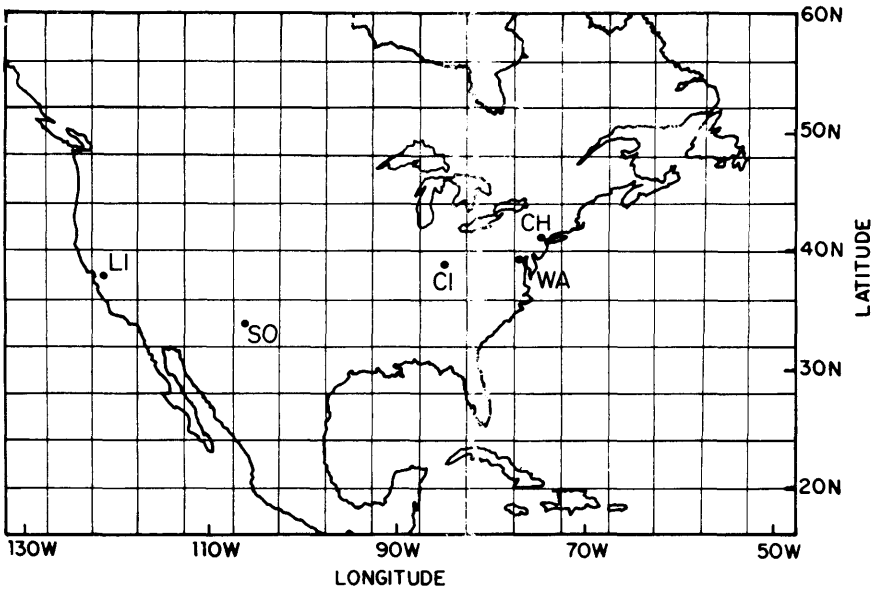

Fig. 1. 4° × 5° horizontal grid of the CTM. The edges of the figure delineate the boundaries of the North America window. Time series of observed ^{222}Rn concentrations extending for more than 1 year are available from Chester, New Jersey (CH); Washington, D.C. (WA); Cincinnati, Ohio (CI); Socorro, New Mexico (SO); and Livermore, California (LI).

planetary boundary layer. A number of investigators have used observed vertical profiles of ^{222}Rn to calibrate 1-d eddy diffusion models of atmospheric transport (Jacobi and Andre, 1963; Beck and Gogolak, 1979; Liu et al., 1984). However vertical profiles extending above the boundary layer are few and scattered (Liu et al., 1984), and difficult to interpret climatologically because the vertical distribution of ^{222}Rn is likely to be strongly affected by local fluctuations in convective activity. Ground-based measurements provide at this time a better data base for evaluating climatological transport models; long-term records of ^{222}Rn concentrations are available from a number of sites around the world (Lambert et al., 1982; Gesell, 1983).

Time series of ^{222}Rn concentrations extending for at least 1 year are available from 5 sites in the United States (Fig. 1). The main features of the data have been reviewed by Gesell (1983). The concentrations are maximum at night, and minimum at midday, following the diurnal cycle of mixed layer growth and decay. Seasonal variations of a factor 2 to 4 are also observed but the phase differs from site to site. At Socorro and Livermore, the concentrations are lowest in spring and summer, when dry convective activity is maximum (Wilkening, 1959; Lindeken, 1966). By contrast, in the northeastern United States the lowest concentrations are observed from February to May (Lockhart, 1964; Gold et al., 1964; Fisenne, 1985). Inhibition of the ^{222}Rn source by soil freezing could explain the low concentrations observed in winter (George, 1981). The low concentrations in April and May may be due to frequent wet convection (Juzdan et al., 1985), intrusions of oceanic air (Lockhart, 1964), or reduced ^{222}Rn emission, as discussed below.

We compare in this paper the ^{222}Rn distributions simulated with the CTM to observations from the United States sites. Meteorological input to the CTM is provided by the 4° × 5° GISS GCM II (Hansen et al., 1983), which includes resolution of the diurnal cycle. The same GCM meteorology is used as in the previous studies by Prather et al. (1987) and Jacob et al. (1987). However the spatial grid of the CTM is finer than in these previous studies (4° × 5° versus 8° × 10°), and all transport processes (in particular convection) are resolved over 4-hour time steps. The main elements of the CTM are reviewed in Section 2. Simulation of ^{222}Rn emission is discussed in Section 3. Model results

are compared to observations in Sections 4–6, with focus on the Chester time series (Section 4), other time series in the United States (Section 5), and vertical profiles (Section 6). Concluding remarks are in Section 7.

2. Simulation of atmospheric transport

The CTM solves the 3-d continuity equation of tracer concentration over 4-hour time steps, using the grid and the meteorology of the GISS GCM II (Hansen et al., 1983). The horizontal resolution is 4° latitude × 5° longitude (Fig. 1). There are 9 layers in the vertical, distributed from the surface to 10 mb along sigma coordinates; the 3 lower layers extend to approximately 500, 1200, and 2600 m above ground level. A 1-year record of GCM output is used as input to the CTM including (1) 4-h mean winds at the boundaries of each gridbox; (2) 4-hourly surface pressures, 4-h mean mixed layer depths, and 4-h totals of convective events (separately shallow wet, deep wet, and dry) in each grid square column; (3) 5-day mean temperatures in each surface gridbox; and (4) 5-day means of the detailed pattern of convective frequencies (shallow wet, deep wet, and dry convection events between individual pairs of vertical layers in each grid square column). The mixed layer depth is defined as the top model layer to which dry convective instability initiated from the surface extends.

The computational structure of the CTM has been described in detail by Prather et al. (1987). Simulation of convective transport follows the scheme used in the GCM to transport momentum, sensible heat, and moisture (Hansen et al., 1983). When a column of air is unstable with respect to a dry adiabat (dry convection), the air is mixed uniformly within the column. When a column of air is unstable with respect to a wet adiabat (wet convection), 50% of the air in the lowest layer of the column is moved directly to the highest layer at which it is stable, with no entrainment of air from intermediate layers; this upward flux is followed immediately by subsidence over intermediate layers as necessary to conserve mass. The convective adjustment of tracer concentration is computed in the CTM at each 4-h time step using the sum of convective events recorded by the GCM over the last 4 h, and apportioning this sum among pairs of vertical layers following the 5-day average wet and dry convection statistics. Dry convection initiated at the surface is computed separately by mixing uniformly the air from the surface up to the mixed layer depth averaged over the past 4 h (if the depth is a fractional number of layers due to the 4-hour averaging of GCM output, then only the appropriate part of the uppermost layer is mixed). This separate treatment of surface-based dry convection provides some resolution of the diurnal cycle of mixed layer growth and decay.

Advection is computed by an upstream method with conservation of first- and second-order moments of concentration (Prather, 1986). In this manner the internal distribution of ^{222}Rn within a gridbox is described as a second-order polynomial in 3-dimensional space. Conservation of moments significantly reduces numerical diffusion compared to conventional upstream advection (Prather, 1986); it also provides useful subgrid resolution to describe the vertical gradient of ^{222}Rn between the ground and the middle of the surface gridbox, and the horizontal gradient of ^{222}Rn within coastal grid-boxes. At each time step the moments in the surface gridbox are adjusted for ^{222}Rn emission as described in the next section. The moments are not conserved during convection, i.e., air parcels transported vertically by convection are assumed to mix horizontally and vertically over the scale of the gridbox (Prather et al., 1987).

The CTM simulation is conducted over a North America "window" of the global GCM grid. In a window calculation the tracer concentrations are computed only for a portion of the global grid, with fixed concentrations assumed at the boundaries (Prather et al., 1987). We adopt 47.5°W and 132.5°W as E–W boundaries, and 60°N and 16°N as N–S boundaries (Fig. 1). These boundaries are located over oceans and polar regions, where ^{222}Rn levels are considerably lower than over North America (Gesell, 1983). Background ^{222}Rn concentrations of 0.1 picoCuries per standard cubic meter of air (pCi/SCM) are assumed at all boundaries (pCi/SCM is a mixing ratio unit, with 1 pCi/SCM = 6.6×10^{-22} molecules of ^{222}Rn per molecule of air). Simulated surface concentrations over the United States are insensitive to the

choice of boundary conditions. The simulation is conducted for 13 model months, starting from initially low concentrations on 1 December. The results presented below are from the last 12 months of the simulation (1 January to 31 December). The details of initial conditions are unimportant since 99.6% of the ^{222}Rn initially present on 1 December would have decayed by 1 January.

The only significant sink for ^{222}Rn in the atmosphere is radioactive decay. The solubility of ^{222}Rn in water is 2.2×10^{-2} moles l^{-1} atm^{-1} (Chemical Rubber Company, 1986), sufficiently low that precipitation scavenging can be neglected (Giorgi and Chameides, 1985). Simultaneous measurements of ^{222}Rn in surface air and in rainwater over Japan (Miyake et al., 1980) indicate concentrations that are roughly consistent with the partitioning expected from the solubility, confirming that precipitation scavenging can be ignored in the computation of the ^{222}Rn budget.

3. Simulation of ^{222}Rn emission

Radon-222 is a daughter of ^{226}Ra, which is an ubiquitous constituent of crustal material. Emission of ^{222}Rn to the atmosphere follows from radioactive decay of ^{226}Ra in soil and upward transport of ^{222}Rn through the soil gas to the surface. The flux of ^{222}Rn depends on the ^{226}Ra abundance in soil, on the physical properties of the soil, and on meteorological conditions. Estimates of the global mean ^{222}Rn flux from soils range from 0.75 atoms cm^{-2} s^{-1} (Wilkening et al., 1975) to 1.2 atoms cm^{-2} s^{-1} (Turekian et al., 1977). Emissions from water surfaces are two orders of magnitude lower (Wilkening and Clements, 1975) and can be neglected as a source of ^{222}Rn over continents.

Emission of ^{222}Rn by evapotranspiration from vegetation must be small compared to soil emission, considering typical evapotranspiration rates and the low solubility of ^{222}Rn in water (Schery et al., 1984). Martell (1985) has argued that evapotranspiration could enhance 5–10 times the flux of ^{222}Rn compared to a bare soil surface, citing as evidence field studies by Pearson and Jones (1966), Guedalia et al. (1970), and Mattsson (1970), but none of these field studies actually provides convincing support for such a claim. Pearson and Jones (1966) reported a preliminary set of measurements suggesting that ^{222}Rn emissions from a corn canopy were higher than from the soil underneath, but later experiments failed to confirm this result (unpublished data from Pearson cited by Mattsson, 1970). Guedalia et al. (1970) found that ^{220}Rn emissions from a mature wheat field were 1.5 to 3 times higher than from adjacent grass, but as they pointed out this variation could be explained by differences in the physical states of the soils (in particular the plowing of the wheat field). Mattsson (1970) measured a seasonal increase in ^{222}Rn concentrations from spring to summer at sites in Finland, which Martell (1985) attributed to the fuller canopy in summer; however Mattsson (1970) argued that the low ^{222}Rn concentrations observed in spring were caused instead by a rise in the water table to near ground level, inhibiting ^{222}Rn emission by clogging of the soil pores. We assume in the CTM that emission from vegetation is negligible, so that soils provide the only source of ^{222}Rn to the atmosphere.

The ^{226}Ra content of soils in the United States ranges from 0.2 to 4 pCi g^{-1} of soil (Myrick et al., 1983). A detailed map of ^{226}Ra soil concentrations is available for the western United States extending east to 110°W (Moed et al., 1984). When averaged over the 4° × 5° CTM grid, the concentrations indicated by this map range from a low value of 0.4 pCi g^{-1} in the Oregon/Washington gridbox (centered at 46°N, 120°W) to a high value of 1.1 pCi g^{-1} in the central California gridbox (centered at 38°N, 120°W), i.e., a factor of 3 variation. Quantitative interpretation of ^{226}Ra soil concentrations in terms of ^{222}Rn emission is however difficult because only a fraction of the decaying ^{226}Ra atoms releases ^{222}Rn to the soil gas. This fraction is determined mainly by the location of ^{226}Ra within the soil grains, and may vary from 10% to 50% depending on soil type (Barretto et al., 1972). For lack of better information, we assume in the CTM that all soils in North America have equal potential for ^{222}Rn emission. A standard emission flux $F_0 = 1$ atom cm^{-2} s^{-1} from land areas is adopted, intermediate between the world-wide estimates of Wilkening et al. (1975) and Turekian et al. (1977)

(conversion to pCi units: 1 atom cm^{-2} s^{-1} = 57×10^{-6} pCi cm^{-2} s^{-1}). The land area fraction in coastal gridboxes is computed from a $1° \times 1°$ land-use map (Matthews, 1983).

Changes in surface pressure generate a net flow of air through the soil, which may cause the emission flux $F(t)$ in a particular gridbox to depart from the standard value F_0 (assumed to be the diffusion-limited flux). The effect of changes in surface pressure on ^{222}Rn emission has been measured by Clements and Wilkening (1974) and by Schery and Gaeddert (1982), and 1-d flow models have been proposed by Clements and Wilkening (1974) and by Edwards and Bates (1980). We adopt in the CTM the following parameterization:

$$F(t+\Delta t) = F(t)\,e^{-\Delta t/\tau} + F_0\left(1 - k\frac{\Delta P}{\Delta t}\right)(1 - e^{-\Delta t/\tau}), \quad (1)$$

where Δt is the CTM time step, $\Delta P/\Delta t$ is the surface pressure gradient (obtained from GCM surface pressures at times t and $t+\Delta t$), and k and τ are fixed coefficients characterizing the effect of pressure forcing and the relaxation time of the soil column, respectively. We find that $k = 1.1$ h mb^{-1} and $\tau = 8$ h yield a source function that is reasonably consistent with the model results of Clements and Wilkening (1974) and Edwards and Bates (1980).

The standard flux F_0 in the CTM is reduced under freezing conditions to simulate the clogging of the soil pores by ice. The effect of soil freezing on ^{222}Rn emission is clearly apparent in the 3-year time series of ^{222}Rn emission flux measurements at Chester (George and Breslin, 1979; George, 1980, 1981). Our analysis of the Chester data indicates that the average flux decreased from 3.3 ± 1.5 atoms cm^{-2} s^{-1} under non-freezing conditions ($n = 116$) to 1.1 ± 1.0 atoms cm^{-2} s^{-1} under freezing conditions ($n = 13$). On the basis of this result we assume in the CTM that F_0 decreases by a factor of 3 when the 5-day mean temperature of a surface gridbox falls below 0°C. The ^{222}Rn fluxes measured at Chester are actually 3 times higher than our assumed model values for F_0, but this discrepancy appears to be caused by locally high ^{226}Ra soil concentrations at Chester; fluxes measured at other sites in New Jersey and New York are much lower, of order 1 atom cm^{-2} s^{-1} (George, 1980).

The effect of soil moisture on ^{222}Rn emission is poorly understood, and conflicting results are reported in the literature (Guedalia et al., 1970; Tanner, 1980; Stranden et al., 1984; Schery et al., 1984). The ^{222}Rn fluxes measured at Chester show no significant correlation with rainfall (George and Breslin, 1979; George, 1980; George, 1981), and there is no significant difference in the flux between wet and dry periods (Fig. 2), suggesting that high soil moisture has little effect on ^{222}Rn emission at that site. On the basis of the Chester data we assume in the CTM that ^{222}Rn emission is independent of soil moisture.

Emission of ^{222}Rn in a CTM gridbox is accompanied by adjustment of the moments of ^{222}Rn concentration. The first-order vertical moment of concentration (vertical slope) is increased by the amount of ^{222}Rn emitted at the bottom of the gridbox (Prather et al., 1987). The horizontal moments of ^{222}Rn emission are added to the corresponding moments of ^{222}Rn concentration. Simulation of ^{222}Rn emission using first- and second-order moments is illustrated in Fig. 3 for the Washington, DC gridbox. The land fraction of this gridbox (computed from the $1° \times 1°$ land-use map) is 45%, with the land distribution shown in Fig. 3a. Assuming non-freezing conditions, and constant surface pressure, the spatially averaged mean flux from the gridbox is $F = 0.45$ atoms cm^{-2} s^{-1}. Decomposition into the orthogonal polynomials of the second-order moments method (Prather, 1986) yields the following expression for the spatial distribution of the flux within the gridbox:

$$F(x,y,z) = 0.45 - 0.66(2x-1) + 0.11(6x^2 - 6x + 1) + 0.26(2y-1) + 0.094(6y^2 - 6y + 1) - 0.023(2x-1)(2y-1) - 0.45(2z-1), \quad (2a)$$

with

$$x = |X - X_0|/\Delta X, \quad y = |Y - Y_0|/\Delta Y, \quad z = Z/Z_T, \quad (2b)$$

where X, Y, Z are the longitude, latitude, and altitude variables, respectively, (X_0, Y_0) are the coordinates of the SW corner of the gridbox ($X_0 = 77.5°$W, $Y_0 = 36°$N), Z_T is the altitude at

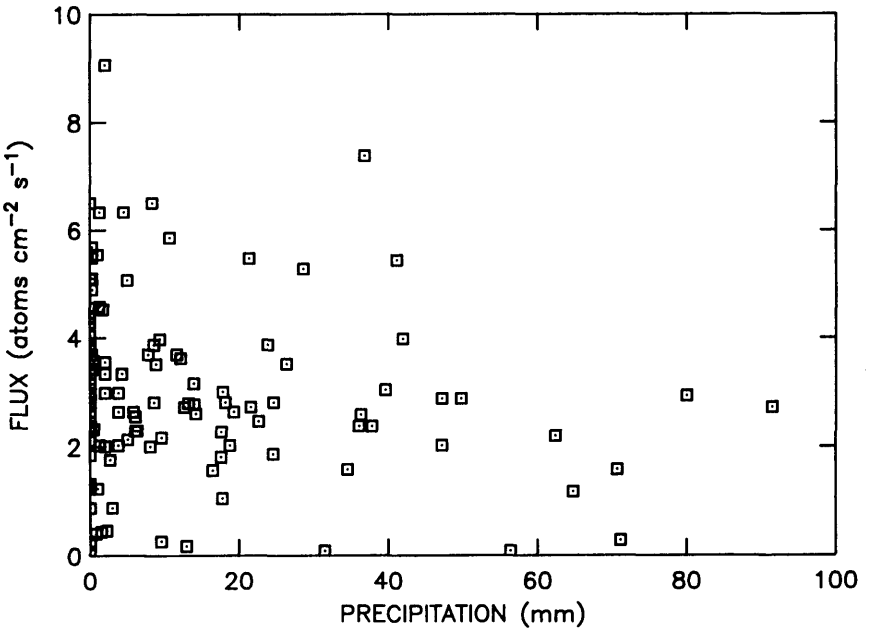

Fig. 2. Observed ^{222}Rn emission flux versus precipitation at Chester. The ^{222}Rn fluxes are 3-day average values and are plotted against the amount of precipitation which fell during the corresponding period. The correlation coefficient between ^{222}Rn emission flux and precipitation is $r = -0.10$ ($n = 129$). The mean flux for dry periods is 2.8 ± 1.3 atoms cm^{-2} s^{-1} ($n = 40$), and the mean flux for wet periods is 3.0 ± 1.7 atoms cm^{-2} s^{-1} ($n = 89$). Data are taken from George and Breslin (1979) and George (1980, 1981).

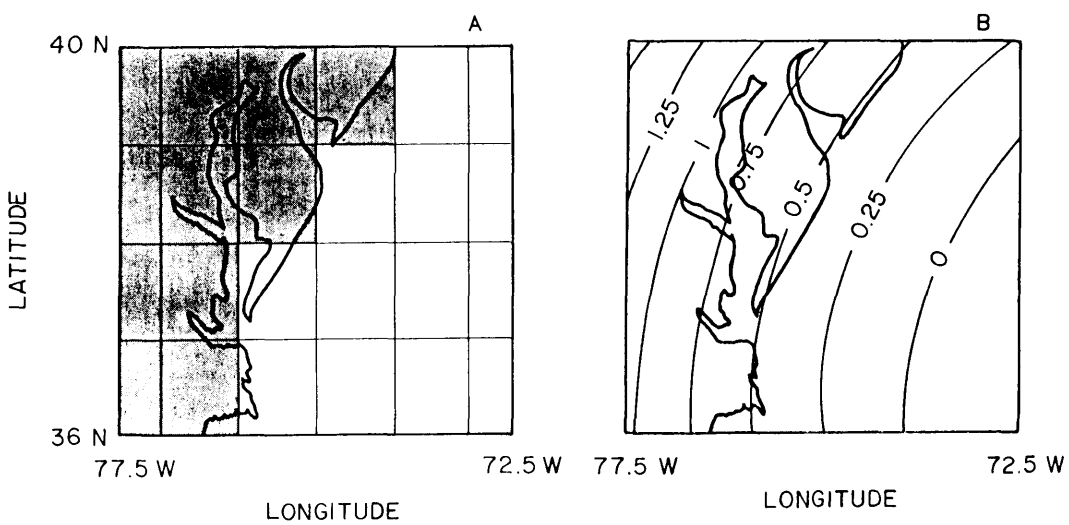

Fig. 3. (A) Land area (shaded) of the Washington, D.C. gridbox, as obtained from the $1° \times 1°$ land-use map (Matthews, 1983). (B) Horizontal distribution of ^{222}Rn emission (atoms cm^{-2} s^{-1}) computed using first- and second-order moments (eq. (2), with $z = \frac{1}{2}$).

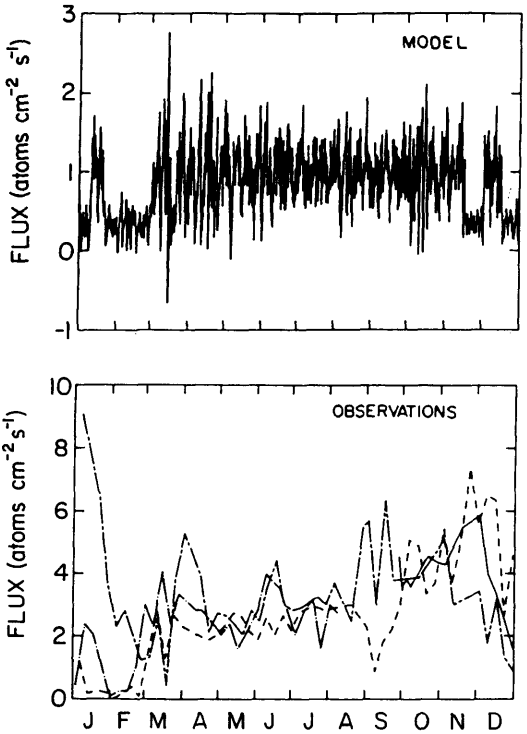

Fig. 4. Time series of ^{222}Rn emission fluxes at Chester. Model values (top panel) are compared to observations for September 1978–August 1981 (bottom panel). The observations are 3-day average values, taken from George and Breslin (1979) and George (1980, 1981). The 4 calendar years of observations are superimposed: 1978 (solid), 1979 (dashes), 1980 (solid-dashes), and 1981 (solid-dots).

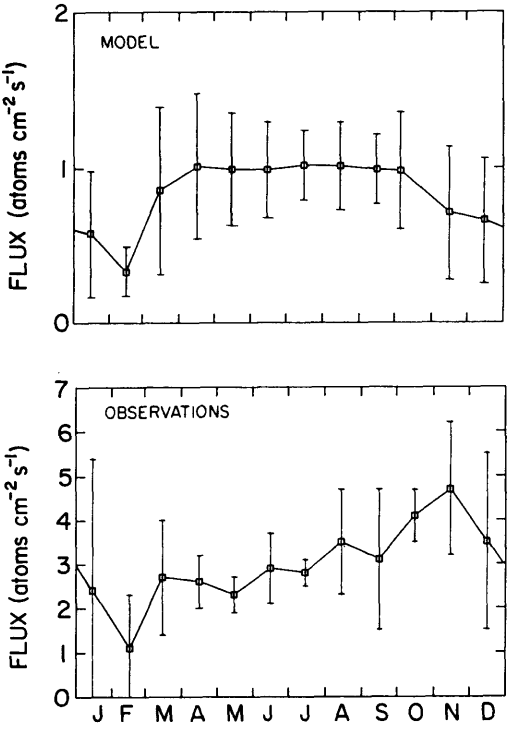

Fig. 5. Monthly mean emission fluxes at Chester ± standard deviations. Model values (top panel) are compared to observations for September 1978–August 1981 (bottom panel). Observations are taken from George and Breslin (1979) and George (1980, 1981).

the top of the gridbox, and the horizontal dimensions of the gridbox are $\Delta X = 5°$ and $\Delta Y = 4°$. At each time step an amount $F\Delta t$ of ^{222}Rn is added to the concentration in the surface gridbox. As shown in Fig. 3b, eq. (2a) gives the desired contrast between land and ocean. Compared to assuming a uniform source of 0.45 atoms cm^{-2} s^{-1}, the root-mean-square error on ^{222}Rn emission in the gridbox is decreased from 0.50 to 0.31 atoms cm^{-2} s^{-1}.

We compare in Fig. 4 the CTM emission fluxes at Chester to the 3-year time series of observed values. Observed fluxes at Chester are a factor of 3 higher than in the CTM, but this difference reflects a local anomaly as discussed above. Emissions are low in winter (particularly in February) because of soil freezing. Two very high flux values are observed in January, probably due to thawing of the soil and release of ^{222}Rn trapped in the soil gas. The high-frequency fluctuations of the flux in the CTM are caused by changes in surface pressure; they show no significant diurnal cycle, and little persistence beyond 1 day. Mean monthly fluxes are plotted in Fig. 5, for both CTM and observations. The monthly mean fluxes in the CTM are constant from April to October, but the observations show a gradual increase during that period for which we have no clear explanation. Possibly, the increase could result from lower precipitation in the fall than in the spring (Juzdan et al., 1985), and hence lower soil moisture, but the lack of a simple anticorrelation between observed ^{222}Rn fluxes and rainfall does not encourage this hypothesis. Without an explanation, we cannot presume that this seasonal variation is representative of other locations, and therefore choose not to include it in the CTM source function. The unresolved seasonal trend must however be kept in mind as a

source of uncertainty when comparing model results to observations.

4. Comparison with observations at Chester

The record of ^{222}Rn concentrations at Chester is by far the most extensive. Measurements were made round-the-clock 10 m above ground in an open field, and data from July 1977 to November 1983 are available as a continuous time series of 3-hour average concentrations (Harley, 1978, 1979; Fisenne, 1980, 1981, 1982, 1984, 1985).

We compare in Fig. 6 the simulated time series of ^{222}Rn concentrations at Chester to observations for 1978 (other years look similar). Remarkably, the observed ^{222}Rn concentrations show little dependence on wind direction (Table 1), even though the site is only 80 km from the coast. The variance of the observations is dominated by a strong diurnal cycle, which is also present in the CTM but is much weaker. Mean ^{222}Rn concentrations as a function of time of day, for each season, are shown in Fig. 7. Concentrations are lowest at midday, when the depth of the mixed layer is maximum, and highest at night, when vertical mixing is suppressed. The amplitude of the diurnal cycle is largest in summer, and smallest in winter, reflecting the seasonal difference in turbulent energy derived from solar heating. The concentrations simulated by the CTM are in good agreement with observations at midday, but are systematically low at night, underpredicting the amplitude of the diurnal cycle.

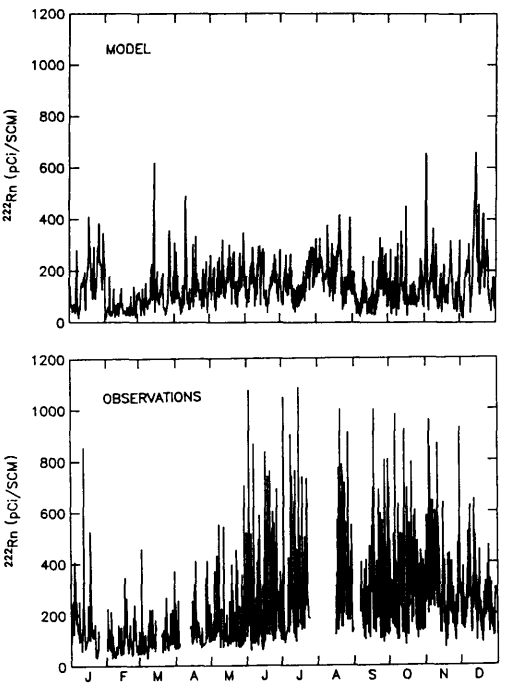

Fig. 6. Time series of ^{222}Rn concentrations at Chester. Model results (top panel) are compared to observations for 1978 (bottom panel). Observations are taken from Harley (1978, 1979).

The failure of the model to reproduce night-time observations may be traced directly to the GCM vertical resolution of the lowest layer. The GCM (and hence the CTM) does not resolve the thermal stratification near the ground and the sharp ^{222}Rn concentration gradient that forms as a result. Moses et al. (1960) measured ^{222}Rn vertical profiles over a grassy field in Illinois in summer, and found that night-time concentrations at 6 m above ground were up to a factor of 10 times higher than at 40 m above ground. In comparison, the vertical moment associated with ^{222}Rn emission in the CTM can produce at most a factor of 2 gradient between the ground and the middle of the surface gridbox ($\approx$250 m altitude). The night-time discrepancy between model and observations is largest in summer, probably

Table 1. *Mean ^{222}Rn concentrations observed at Chester for different wind direction sectors*

Sector	*n*	Concentration (pCi/SCM)
0–90°	20	236 ± 93
90–180°	49	228 ± 92
180–270°	34	277 ± 94
270–360°	105	248 ± 94

Mean concentrations ± standard deviations are computed from the 1977–1983 time series of observations, restricted to May–October and averaged over 24-h periods. Restriction to May–October removes the influence of soil freezing, and use of 24-h averages removes the diurnal cycle associated with vertical mixing. We find that the concentrations associated with the 180–270° sector are significantly higher than those associated with the 90–180° sector (95% confidence limit). Other pairs of sectors show no significant differences. Concentrations are taken from Fisenne (1985) and references therein; wind directions are taken from Juzdan et al. (1985) and references therein.

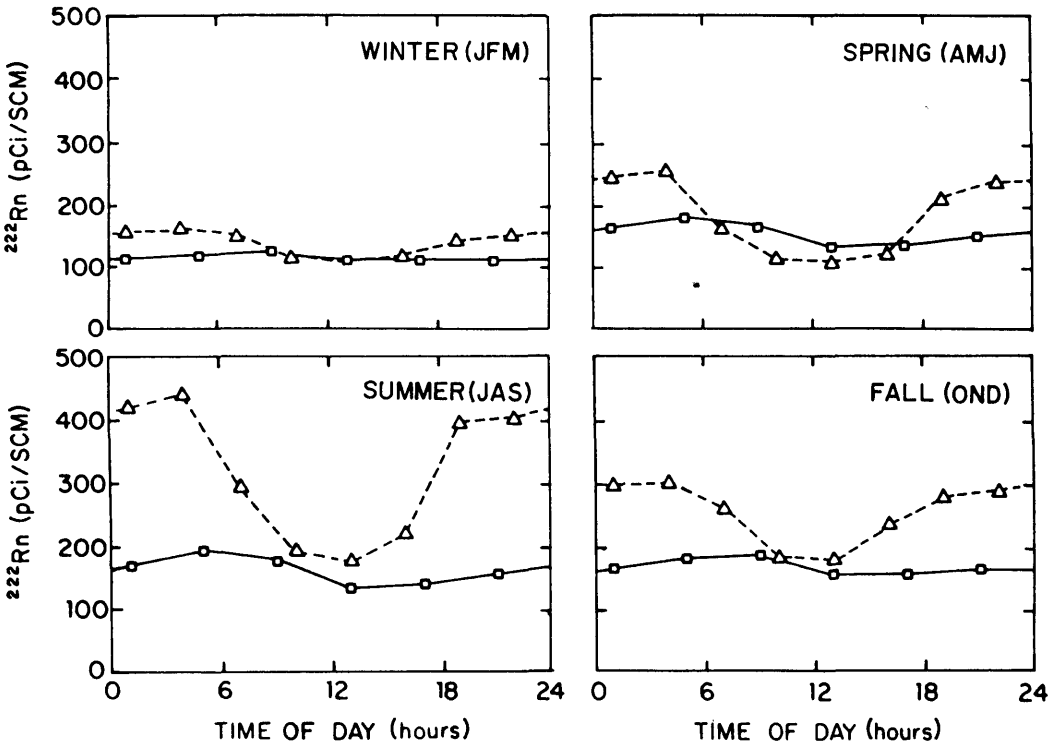

Fig. 7. Seasonally averaged ^{222}Rn concentrations at Chester, as a function of time of day. Model results (solid lines) are compared to observations for 1977–1983 (dashed lines). Observations are taken from Fisenne (1985) and references therein.

because wind speeds are minimum in that season and mechanical mixing of the surface layer is therefore particularly slow.

Vertical mixing of surface air is considerably enhanced during the daytime because of turbulence generated by buoyancy. The measurements of Moses et al. (1960) indicate no significant gradient in daytime ^{222}Rn concentrations between 6 and 40 m, suggesting that the Chester measurements at 10 m altitude are representative of a mixed layer sufficiently deep to be resolved with the CTM grid. The good agreement between simulated and observed concentrations at midday is indeed evidence that the CTM gives a reasonable simulation of boundary layer convection, considering the sensitivity of the simulated ^{222}Rn concentrations to the intensity of convective mixing. This sensitivity can be illustrated by considering two 1-dimensional steady-state cases in which a constant flux of ^{222}Rn is emitted from the surface ($F = 1$ atom cm^{-2} s^{-1}). If the emitted ^{222}Rn were confined to the lowest CTM layer ($\approx$500 m thick), then steady-state ^{222}Rn concentrations would reach 1400 pCi/SCM at the surface. If the ^{222}Rn emissions were mixed to a height of 255 mb (CTM layer 6), the concentration would be only 48 pCi/SCM. In our simulation, the yearly mean ^{222}Rn concentration at 1300 LT (local time) is 136 pCi/SCM, in very close agreement with the mean value of 143 pCi/SCM computed from the 7 years of observations. Such a close agreement must however be regarded as fortuitous in view of the uncertainty of the source, as discussed above.

Fig. 8 shows the 90-day running averages of observed concentrations at 1300 LT, for each of the 7 years of observations, and the corresponding concentrations simulated with the CTM. Use of 90-day running average statistics allows to focus on seasonal variations, filtering out anomalous months. Superimposition of the 7 years of data gives a measure of the interannual variability. Model and observations are usually in good agreement, but inspection of the seasonal

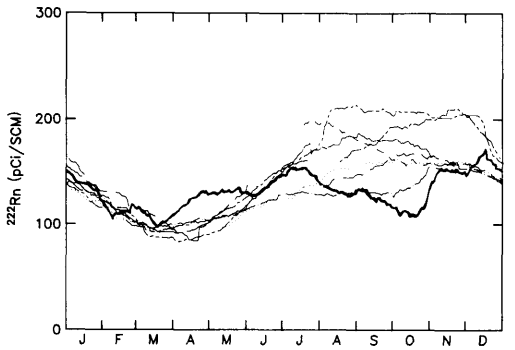

Fig. 8. 90-day running average 1300 LT concentrations at Chester. Model results (bold line) are compared to observations for 1977–1983 (thin lines). The 7 calendar years of observations are superimposed: 1977 (short dashes), 1978 (long-short dashes), 1979 (dashes-dots), 1980 (long-short-short dashes), 1981 (long dashes), 1982 (dots), 1983 (solid). Observations are taken from Fisenne (1985) and references therein.

trend reveals two significant discrepancies which lie beyond the range of interannual variability of the observations: (1) overprediction of concentrations in April and May, and (2) underprediction of concentrations in September and October. The possibility of an unresolved seasonal trend in the ^{222}Rn source cannot be excluded (Fig. 5), but we seek instead a meteorological explanation. Examination of the local GCM meteorology indicates excessive rainfall in April–July, and insufficient rainfall in September–November (Fig. 9); from the lower panel of Fig. 9 we see that convection in the GCM is suppressed during rainy months, and enhanced during dry months. The rainfall anomaly in the GCM can therefore qualitatively explain the observed discrepancies in the daytime ^{222}Rn concentrations. Although rainfall in the GCM is usually associated with local moist convective activity, excessive rainfall saturates the soil with moisture and prevents the development of dry convection. By contrast, drought conditions allow vigorous dry convection due to the lack of ground moisture available for evaporation.

The excessive GCM rainfall in spring and early summer can be reduced by adjusting the parameterization of groundwater storage to increase runoff (D. Rind, GISS, personal communication, 1988). Correction of the GCM drought is less straightforward. The drought is particularly severe over the New Jersey/New York gridbox, but extends over most of the

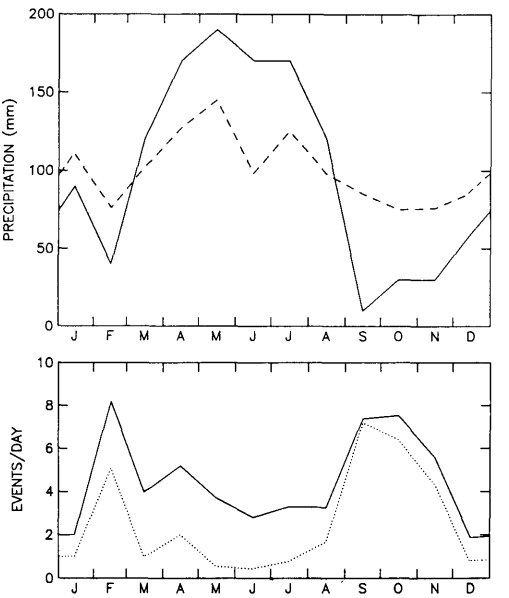

Fig. 9. Monthly total precipitation at Chester (top panel). The GCM results (solid line) are compared to mean observations for 1978–1984 (dashed line) as reported by Juzdan et al. (1985). The bottom panel shows monthly mean GCM frequencies of convective events in the Chester grid square column; sum of wet and dry convection (solid line) and dry convection only (dotted line). Convective events are recorded as hourly diagnostics, therefore the maximum frequency (corresponding to continuous convective mixing) is 24 events/day. Wet convection events are counted as half-events because only half of the lower gridbox is ventilated (see Section 2 of the text).

eastern United States where September precipitation is substantially less than normal (Fig. 10). A major factor in the drought appears to be a northeastward displacement of the Bermuda High in summer (Fig. 11), which suppresses the northward flow of moist air from the Gulf of Mexico to the North American continent. As the summer progresses the central and eastern United States become gradually desertified, starting from the Gulf Coast and propagating towards the north. Evaporation from the Gulf of Mexico is not the factor limiting rainfall; a GCM experiment with sea surface temperatures in the Gulf raised by 2°C showed no improvement in the precipitation pattern (G. L. Russell, GISS, personal communication, 1988). The displacement of the Bermuda High may be a consequence of tropical meteorology, i.e, the summertime ITCZ in the GCM is 5–10° too far north (C. M.

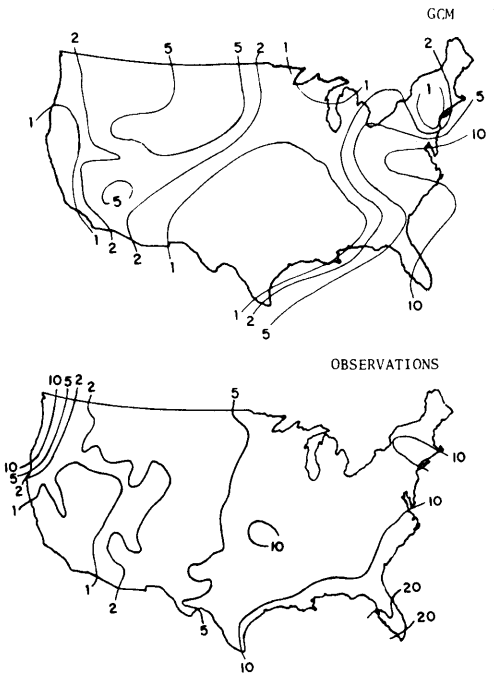

Fig. 10. September rainfall (cm) over the United States. The GCM results (top) are compared to climatological observations (bottom).

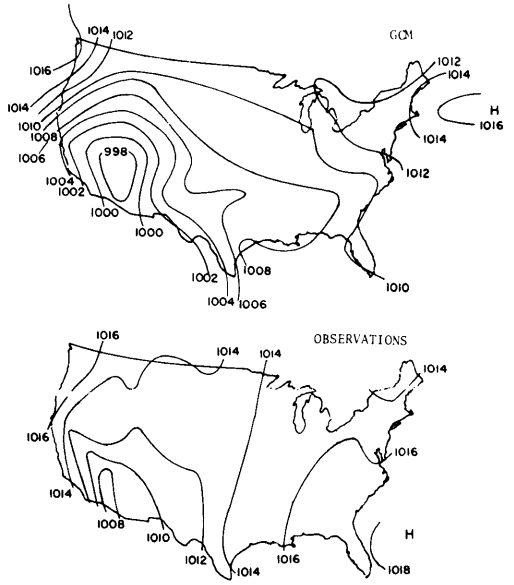

Fig. 11. Mean July MSL pressures (mb) over the United States. The GCM results (top) are compared to climatological observations (bottom).

Spivakovsky, Harvard University, personal communication, 1988) which might cause a similar diplacement of the subtropical highs. Significant improvement in the location of the Bermuda High was achieved in a GCM experiment using a new parameterization of moist convective mass fluxes aimed at improving tropical convection (Del Genio and Yao, 1988).

Changes in ^{222}Rn concentrations at Chester from day to day should follow mainly from changes in convective activity; therefore, an autocorrelation analysis of the time series of concentrations gives a measure of the persistence of weather patterns in the region. We apply here such an analysis to the residuals relative to the 90-day running average 1300 LT concentrations (use of the residuals removes the seasonal trend). The normalized autocorrelation coefficient $r(\tau)$ at time lag τ is defined as follows:

$$r(\tau) = \frac{T}{T-\tau} \frac{\sum_{\tau}^{T} R(t)\,R(t-\tau)}{\sum_{0}^{T} R^2(t)}, \qquad (3)$$

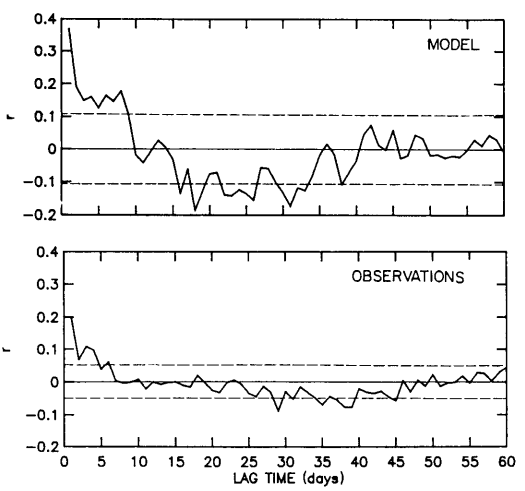

Fig. 12. Autocorrelogram of 1300 LT ^{222}Rn concentrations at Chester: normalized autocorrelation coefficient (r) versus time lag. Model results (top panel) are compared to observations (bottom panel). The dashed lines represent 95% confidence limits ($\pm 2/\sqrt{n}$; Chatfield, 1984).

where $R(t)$ is the residual at time t, and t is a discrete time variable taking the values 0, 1, 2, ... T days. There are $T = 365$ days of data in the model simulation, and $T = 1870$ days in the

observations (after removal of periods with sparse data). The variance of the data set,

$$\frac{1}{T}\sum_{0}^{T} R^2(t),$$

is 8500 $(\text{pCi/SCM})^2$ in the model and 4100 $(\text{pCi/SCM})^2$ in the observations. Autocorrelograms for the simulated and observed time series are compared in Fig. 12. We find significant autocorrelation to about 8 days in the model, and to 4–6 days in the observations. The model captures well the sharp drop in the autocorrelation between day 1 and day 2, and the relatively flat shoulder between day 2 and day 4. The wider shoulder in the model indicates that GCM weather systems in the northeastern United States may be slightly too persistent. No strong periodicities aside from diurnal and yearly are found either in the model or in the observations; weak periodicities are apparent at 15–35 days in the model, and at 30–45 days in the observations, but these are at the limit of being significant.

5. Comparison with observations at other sites

Observed ^{222}Rn concentrations at other United States sites are available as monthly mean values for particular times of the day. The monthly means correspond to 12 years of data at Washington, D.C., 4 years at Cincinnati, 6 years at Socorro, and 1 year at Livermore. We focus our attention on the daytime data, when the measured surface concentrations are most representative of the mixed layer above. The CTM results for each site are compared to observations in Fig. 13. The lower panels in the figures show the monthly mean convection frequencies in the corresponding GCM gridbox.

The observed time series at the 2 eastern United States sites, Washington and Cincinnati, display seasonal trends similar to those at Chester, with low concentrations in the spring and high concentrations in late summer and early fall. At both sites, the model overpredicts the observed concentrations in the spring, and this overprediction coincides with excessive GCM rainfall. By contrast to Chester, however, good agreement is found between model and observations in September and October. A likely explanation is that the GCM drought is less severe over Washington or Cincinnati than it is over Chester (Fig. 10).

High concentrations are observed at Washington during December and January, because soil freezing is uncommon, and these high concentrations are well reproduced by the CTM. However, a major discrepancy is found at Cincinnati in December and January, when simulated concentrations are much higher than observed. Convective activity is weak at that time of year, so that the low observed concentrations are most likely the result of soil freezing; the high values simulated by the model indicate by contrast little effect from soil freezing. Mean January winds over Cincinnati are SW both in the GCM and in the climatological observations. The January freezing isopleth passes to the north of the Cincinnati gridbox in the GCM, but the observed climatological isopleth passes near Cincinnati and extends west at the same latitude (Fig. 14). The overprediction of ^{222}Rn concentrations at Cincinnati may thus be due to prediction of higher than usual temperatures in the Cincinnati gridbox and in the adjacent gridbox to the west.

The seasonal trends of observed concentrations at the two sites in the western United States, Socorro and Livermore, follow largely the seasonal pattern of convective activity (Wilkening, 1959; Lindeken, 1966). The convection frequencies predicted by the GCM at these two sites feature a pronounced difference between strong convective activity in spring and summer (mainly dry convection), and weak convective activity in fall and winter (mostly wet convection). We find that the seasonal trend of ^{222}Rn concentrations at Socorro is reasonably well simulated throughout the year, reflecting the good simulation of dry convection. At Livermore, however, the CTM predicts excessive ^{222}Rn concentrations in the summer months despite vigorous dry convection and a good simulation of the NW onshore flow advecting air from the Pacific Ocean. The high ^{222}Rn concentrations predicted at Livermore are due to offshore advection of continental air from Oregon, following the cyclonic circulation around the heat Low over the southwestern United States; this continental air is then transported from the Pacific Ocean back to the California coast by the NW flow (Fig. 11).

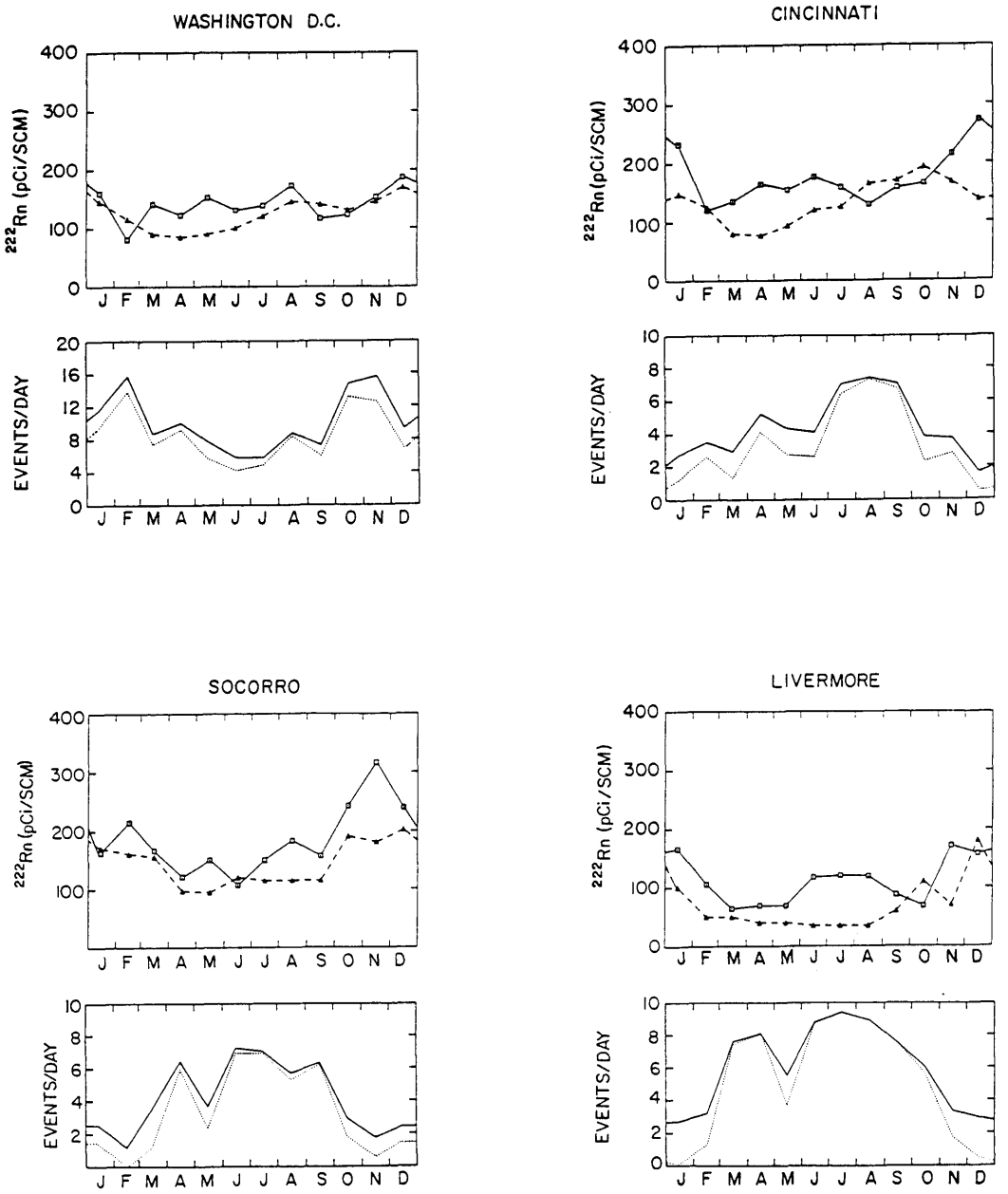

Fig. 13. Monthly mean afternoon ^{222}Rn concentrations at sites in the United States (top panel). Model results (solid lines) are compared to observations (dashed lines). Observations are for 1500 LT at Cincinnati (Gold et al., 1964), "mid-afternoon" at Washington (Lockhart, 1964), 1500 LT at Socorro (Wilkening, 1959), and "afternoon" at Livermore (Lindeken, 1966). The bottom panels show monthly mean GCM frequencies of convective events in the grid square columns corresponding to each site: sum of wet and dry convection (solid lines) and dry convection only (dotted lines) (see legend of Fig. 9 for details).

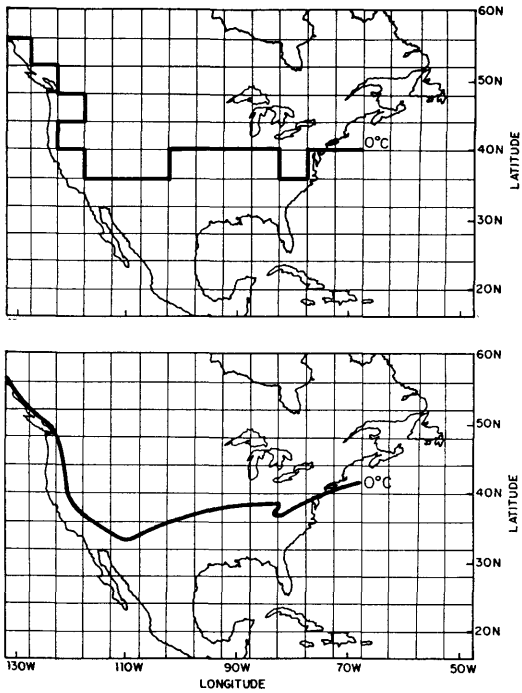

Fig. 14. Mean freezing temperature isopleth for January. The GCM results (top panel) are compared to climatological observations (bottom panel).

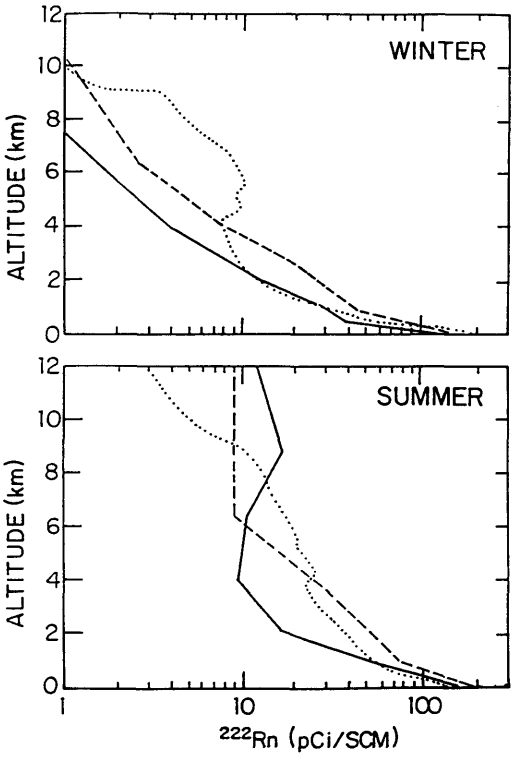

Fig. 15. Mean vertical profiles of ^{222}Rn concentrations in summer and winter. Model results for Chester (solid line) and for Socorro (dashed line) are compared to the mean observed profiles constructed by Liu et al. (1984) (dotted line).

Only 1 year of observations are available from Livermore, therefore it is not clear whether the discrepancy between model and observations is climatologically significant. Offshore transport of continental air during August has been documented during the DYCOMS experiment off the coast of Southern California (120–123°W, 31–34°N), where observed boundary layer ^{222}Rn concentrations ranged from 1.0 to 24 pCi/SCM (Lenschow et al., 1988). The model still predicts excessive concentrations in the DYCOMS sampling region ($\approx$50 pCi/SCM), but the corresponding gridboxes may not be well resolved, being either coastal or adjacent to large continental sources of ^{222}Rn.

6. Comparison with vertical profiles

Only a small number of vertical profiles of ^{222}Rn concentrations over continents are available. Liu et al. (1984) attempted to extract climatological information from the existing data by averaging the concentrations observed at all sites, for each season. We compare in Fig. 15 the vertical profiles simulated by the CTM over Chester and Socorro to the mean winter and summer profiles computed by Liu et al. (1984). In the winter, reasonable agreement is found in the lower troposphere, but above 4 km the CTM concentrations are much lower than indicated by the mean profile. The significance of this discrepancy is not clear however since the mean profile aloft was constructed from only 3 individual profiles. The mean summer profile computed by Liu et al. (1984) is probably more climatologically representative because a larger number of observations are available. The simulated vertical distribution over Socorro in summer agrees well with the mean profile, but at Chester the CTM predicts a layer of high concentrations in the upper troposphere, which is not found in the mean profile. This layer is caused by vigorous dry convection over the western United States, trans-

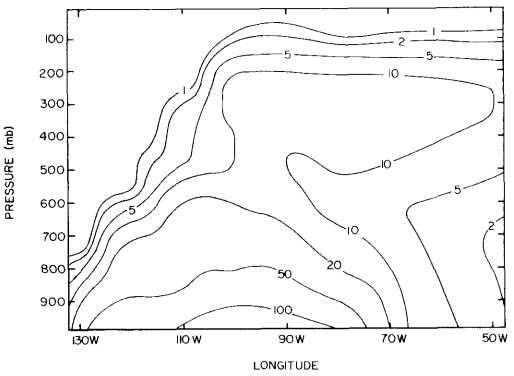

Fig. 16. Monthly mean ^{222}Rn concentrations (pCi/SCM) predicted by the CTM in July at 38°N latitude, as a function of altitude and longitude.

porting ^{222}Rn to 400–300 mb from where it is rapidly advected by the strong upper westerlies (Fig. 16). The eastward transport of ^{222}Rn aloft produces an inversion of ^{222}Rn concentrations at 600–500 mb in summer over most of the eastern United States and over the western Atlantic Ocean. No observed vertical profiles are available from these regions to verify the presence of ^{222}Rn-rich air in the upper troposphere, but the injection of ^{222}Rn to high altitudes over the western United States in summer is consistent with observations of deep dry convection. Measured midday mixing depths over Salt Lake City in July average 5400 m above sea level, compared to 1500–2000 m over the eastern United States (Holzworth, 1967).

7. Conclusions

Simulation of ^{222}Rn surface concentrations over continents provides a stringent test of the ability of a GCM to describe convective mass transport in the boundary layer. We find that a 3-d model based on the meteorology of the GISS GCM II gives in general a reasonable simulation of observations over the United States. Some significant discrepancies are apparent which can be traced to anomalies in the GCM meteorology. In particular the eastern United States in the GCM receive excessive rainfall during the spring and early summer, which suppresses convective activity, and insufficient rainfall in September and October, which allows excessive convective activity. A major factor in the drought appears to be the northeastward shift of the Bermuda High in the GCM. Only one GCM year was used for the ^{222}Rn simulation presented in this paper, but we verified that the same meteorological anomalies were present in other GCM years. Preliminary GCM experiments indicate that the location of the Bermuda High is improved significantly by the use of a new scheme for moist convective mass transport (Del Genio and Yao, 1988). Experiments are in progress at GISS in which the new convection scheme is combined with a modified treatment of ground hydrology aimed at moderating spring rainfall.

8. Acknowledgements

We thank C. M. Spivakovsky (Harvard University) and 3 anonymous reviewers for their useful comments. This work was supported by the National Science Foundation (grants ATM87-19224 and ATM84-13153) and by the National Aeronautics and Space Administration's Tropospheric Chemistry Program (including grant NASA-NAG5-719).

REFERENCES

Barretto, P. M. C., Clark, R. B. and Adams, J. A. S. 1972. Physical characteristics of radon-222 emanation from rocks, soils, and minerals: its relation to temperature and alpha dose. In: *The natural radiation environment II* (eds. J. A. S. Adams et al.). United States Dept. of Commerce, Report CONF-720805, 731–740.

Beck, H. L. and Gogolak, C. V. 1979. Time-dependent calculations of the vertical distribution of ^{222}Rn and its decay products in the atmosphere. *J. Geophys. Res. 84*, 3139–3148.

Chatfield, C. 1984. *The analysis of time series: an introduction, 3rd edition.* Chapman and Hall, p. 63.

Chemical Rubber Company 1986. *Handbook of chemistry and physics, 66th edition* (ed. R. C. Weast), Cleveland, Ohio.

Clements, W. E. and Wilkening, M. H. 1974. Atmospheric pressure effects on ^{222}Rn transport across the earth–air interface. *J. Geophys. Res. 79*, 5025–5029.

Del Genio, A. D. and Yao, M. S. 1988. Sensitivity of a global climate model to the specification of convective updraft and downdraft mass fluxes. *J. Atmos. Sci. 45*, 2641–2668.

Edwards, J. C. and Bates, R. C. 1980. Theoretical evaluation of radon emanation under a variety of conditions. *Health Phys. 39*, 263–274.

Fisenne, I. 1980. Radon-222 measurements at Chester. In: *USDOE rpt. EML-383*, Environmental Measurements Laboratory, U.S. Dept. of Energy, New York, 73–107.

Fisenne, I. 1981. Radon-222 measurements at Chester. In: *USDOE rpt. EML-399*, Environmental Measurements Laboratory, U.S. Dept. of Energy, New York, 213–245.

Fisenne, I. 1982. Radon-222 measurements at Chester. In: *USDOE rpt. EML-411*, Environmental Measurements Laboratory, U.S. Dept. of Energy, New York, 192–227.

Fisenne, I. 1984. Radon-222 measurements at Chester, NJ. In: *USDOE rpt. EML-422*, Environmental Measurements Laboratory, U.S. Dept. of Energy, New York, 115–149.

Fisenne, I. 1985. Radon-222 measurements at Chester, NJ. In: *USDOE rpt. EML-450*, Environmental Measurements Laboratory, U.S. Dept. of Energy, New York, 104–139.

Fung, I., Prentice, K., Matthews, E., Lerner, J. and Russell, G. 1983. Three-dimensional tracer model study of atmospheric CO_2: response to seasonal exchanges with the terrestrial biosphere. *J. Geophys. Res. 88*, 1281–1294.

George, A. C. 1980. Environmental radon and radon daughters. In: *USDOE rpt. EML-383*, Environmental Measurements Laboratory, U.S. Dept. of Energy, New York, 61–72.

George, A. C. 1981. Radon flux measurements. In: *USDOE rpt. EML-399*, Environmental Measurements Laboratory, U.S. Dept. of Energy, New York, 207–212.

George, A. C. and Breslin, A. J. 1979. Environmental radon and radon daughters at Chester. In: *USDOE rpt. EML-367*, Environmental Measurements Laboratory, U.S. Dept. of Energy, New York, 26–38.

Gesell, T. F. 1983. Background atmospheric ^{222}Rn concentrations outdoors and indoors: a review. *Health Phys. 45*, 289–302.

Giorgi, F. and Chameides, W. L. 1985. The rainout parameterization in a photochemical model. *J. Geophys. Res. 90*, 7872–7880.

Gold, S., Barkhau, H. W., Shleien, B. and Kahn, B. 1964. Measurement of naturally occurring radionuclides in air. In: *The natural radiation environment* (eds. J. A. S. Adams and W. M. Lowder), University of Chicago Press, 369–382.

Guedalia, D., Laurent, J.-L., Fontan, J., Blanc, D. and Druilhet, A. 1970. A study of radon 220 emanation from soils. *J. Geophys. Res. 75*, 357–369.

Hansen, J., Russell, G., Rind, D., Stone, P., Lacis, A., Lebedeff, S., Ruedy, R. and Travis, L. 1983. Efficient three-dimensional global models for climate studies: models I and II. *Mon. Weath. Rev. 111*, 609–662.

Harley, J. F. 1977. Radon-222 measurements at Chester. In: *USDOE rpt. EML-347*, Environmental Measurements Laboratory, U.S. Dept. of Energy, New York, 30–65.

Harley, J. F. 1978. Radon-222 measurements at Chester. In: *USDOE rpt. EML-367*, Environmental Measurements Laboratory, U.S. Dept. of Energy, New York, 39–73.

Holzworth, G. C. 1967. Mixing depths, wind speeds and air pollution potential for selected locations in the United States. *J. Appl. Met. 6*, 1039–1044.

Jacob, D. J., Prather, M. J., Wofsy, S. C. and McElroy, M. B. 1987. Atmospheric distribution of ^{85}Kr simulated with a general circulation model. *J. Geophys. Res. 92*, 6614-6626.

Jacobi, W. and Andre, K. 1963. The vertical distribution of radon 222, radon 220 and their decay products in the atmosphere. *J. Geophys. Res. 68*, 3799–3814.

Juzdan, Z. R., Leifer, R. and Pruden, W. 1985. Meteorological data at Chester, NJ. In: *USDOE rpt. EML-450*, Environmental Measurements Laboratory, U.S. Dept. of Energy, New York, 140–158.

Lambert, G., Polian, G., Sanak, J., Ardouin, B., Buisson, A., Jegou, A. and Leroulley, J. C. 1982. Radon cycle and its daughters: applications to the troposphere–stratosphere exchange study. (Cycle du radon et de ses descendants: application a l'etude des echanges troposphère-stratosphère.) *Ann. Geophys. 38*, 497–531.

Lenschow, D. H., Paluch, I. R., Bandy, A. R., Pearson, Jr., R., Kawa, S. R., Weaver, C. J., Huebert, B. J., Kay, J. G., Thornton, D. C. and Driedger III, A. R. 1988. Dynamics and chemistry of marine stratocumulus (DYCOMS) experiment. *Bull. Amer. Met. Soc. 69*, 1058–1067.

Lindeken, C. L. 1966. Seasonal variations in the concentration of airborne radon and thoron daughters. In: *USAEC Rep. UCRL-50007*, University of California Lawrence Radiation Laboratory, Livermore, California, 41–43.

Liu, S. C., McAfee, J. R. and Cicerone, R. J. 1984. Radon 222 and tropospheric vertical transport. *J. Geophys. Res. 89*, 7291–7297.

Lockhart, L. B., Jr. 1964. Radioactivity of the radon-222 and radon-220 series in the air at ground level. In: *The natural radiation environment* (eds. J. A. S. Adams and W. M. Lowder), University of Chicago Press, Chicago, 331–344.

Martell, E. A. 1985. Enhanced ion production in convective storms by transpired radon isotopes and their decay products. *J. Geophys. Res. 90*, 5909–5916.

Matthews, E. 1983. Global vegetation and land use: new high-resolution data bases for climate studies. *J. Climat. Appl. Meteor. 22*, 474–487.

Mattsson, R. 1970. Seasonal variation of short-lived radon progeny, Pb^{210} and Po^{210}, in ground level air in Finland. *J. Geophys. Res. 75*, 1741–1744.

Miyake, Y., Saruhashi, K., Sugimura, Y., Kanazawa, T., Katsuragi, Y. and Uemura, H. 1980. Lead-210 and radon-222 contents of rainwater in Tokyo. In:

The natural radiation environment III (eds. T. F. Gesell and W. M. Lowder), U.S. Dept. of Energy Special Symposium Series 51, CONF 780422, 547–559.

Moed, B. A., Nazaroff, W. W., Nero, A. V., Schweh, M. B. and Van Heuvelen, A. 1984. Identifying areas with potential for high indoor radon levels: analysis of the national airborne radiometric reconnaissance data for California and the Pacific Northwest. Report *LBL-16955*, University of California, Berkeley, California.

Moses, H., Stehney, A. F. and Lucas, Jr., H. F. 1960. The effect of meteorological variables upon the vertical and temporal distributions of atmospheric radon. *J. Geophys. Res. 65*, 1223–1238.

Myrick, T. E., Berven, B. A. and Haywood, F. F. 1983. Determination of concentrations of selected radionuclides in surface soil in the U.S. *Health Phys. 45*, 631–642.

Pearson, J. E. and Jones, G. E. 1966. Soil concentrations of "emanating radium-226" and the emanation of radon-222 from soils and plants. *Tellus 18*, 655–661.

Prather, M. J. 1986. Numerical advection by conservation of second-order moments. *J. Geophys. Res. 91*, 6671–6681.

Prather, M. J., McElroy, M. B., Wofsy, S. C., Russell, G. and Rind, D. 1987. Chemistry of the global troposphere: fluorocarbons as tracers of air motion. *J. Geophys. Res. 92*, 6579–6613.

Schery, S. D. and Gaeddert, D. H. 1982. Measurements of the effect of cyclic atmospheric pressure variation on the flux of ^{222}Rn from soil. *Geophys. Res. Lett. 9*, 835–838.

Schery, S. D., Gaeddert, D. H. and Wilkening, M. H. 1984. Factors affecting exhalation of radon from a gravelly sandy loam. *J. Geophys. Res. 89*, 7299–7309.

Stranden, E., Kolstad, A. K. and Lind, B. 1984. The influence of moisture and temperature on radon exhalation. *Radiat. Prot. Dos. 7*, 55–58.

Tanner, A. B. 1980. Radon migration in the ground: A supplementary review. In: *The natural radiation environment III* (eds. T. F. Gesell and W. M. Lowder), U.S. Dept. of Energy Special Symposium Series 51, CONF 780422, 5-56.

Turekian, K. K., Nozaki, Y. and Benninger, L. K. 1977. Geochemistry of atmospheric radon and radon products. *Ann. Rev. Earth Planet. Sci. 5*, 227–255.

Wilkening, M. H. 1959. Daily and annual courses of natural atmospheric radioactivity. *J. Geophys. Res. 64*, 521–526.

Wilkening, M. H., Clements, W. E. and Stanley, D. 1972. Radon 222 flux measurements in widely separated regions. In: *The natural radiation environment II* (eds. J. A. S. Adams et al.), USERDA CONF-720805, 717–730.

Wilkening, M. H. and Clements, W. E. 1975. Radon 222 from the ocean surface. *J. Geophys. Res. 80*, 3828–3830.